

Autism Spectrum Disorder Classification in Children based on Structural MRI Features Extracted using Contrastive Variational Autoencoder

Ruimin Ma[#], Ruitao Xie[#], Yanlin Wang, Jintao Meng, Yanjie Wei, Wenhui Xi^{*}, and Yi Pan^{*}

Shenzhen Institutes of Advanced Technology, Chinese Academy of Sciences, Center for High Performance Computing, Shenzhen 518055, Guangdong, China

Shenzhen Key Laboratory of Intelligent Bioinformatics, Shenzhen Institute of Advanced Technology, Shenzhen 518055, China

*Corresponding emails: yi.pan@siat.ac.cn, wh.xi@siat.ac.cn

[#] Equally contributed

Abstract

Autism spectrum disorder (ASD) is a highly disabling mental disease that brings significant impairments of social interaction ability to the patients, making early screening and intervention of ASD critical. With the development of the machine learning and neuroimaging technology, extensive research has been conducted on machine classification of ASD based on structural MRI (s-MRI). However, most studies involve with datasets where participants' age are above 5. Few studies conduct machine classification of ASD for participants below 5-year-old, but, with mediocre predictive accuracy. In this paper, we push the boundary of predictive accuracy (above 0.97) of machine classification of ASD in children (age range: 0.92-4.83 years), based on s-MRI features extracted using contrastive variational autoencoder (CVAE). 78 s-MRI, collected from Shenzhen Children's Hospital, are used for training CVAE, which consists of both ASD-specific feature channel and common shared feature channel. The ASD participants represented by ASD-specific features can be easily discriminated from TC participants represented by the common shared features, leading to high classification accuracy. In case of degraded predictive accuracy when data size is extremely small, a transfer learning strategy is proposed here as a potential solution. Finally, we conduct neuroanatomical interpretation based on the correlation between s-MRI features extracted from CVAE and surface area of different cortical regions, which discloses potential biomarkers that could help target treatments of ASD in the future.

INTRODUCTION

Autism spectrum disorder (ASD) is a highly disabling mental disease, the patients of which have impaired social interaction ability, verbal and nonverbal communication deficiencies or other problems.[1] The diagnosis of autism is usually based on behavior scores evaluated by doctors, which may result in inaccurate diagnosis of ASD.[2] Machine learning technology has aroused great attention recently and its role in analyzing medical data has been proven to be effective and efficient in many tasks of computer-aided medical diagnosis, including ASD detection. Accurate machine classification of ASD based on structural MRI (s-MRI) becomes popular and critical recently.[3]

Most researchers conduct machine classification of ASD based on s-MRI collected from the ABIDE.[4, 5] Kong et al. construct an individual brain network to extract connectivity features between each pair of regions of interest from the s-MRI and select top 3000 connectivity features for ASD classification via a deep neural network classifier.[6] Hiremath et al. design a dense model with 4 dense blocks to extract deep features of the s-MRI, which are then combined with the morphometric hand-crafted features, i.e., volume and surface features of different brain parcellations, and fed into a gender specific linear discriminant classifier, to classify ASD from typical control (TC).[7] Gao et al. construct individual-level morphological covariance brain network according to SRI24 atlas[8] and gray matter volume map of each subject's s-MRI, which is used as the input for the ResNet-based classifier for ASD classification.[9] Yang et al. propose three models, 2D Class Activation Mapping (CAM), 3D CAM, and 3D Gradient-weighted CAM with s-MRI as inputs for classifying ASD.[10-12] Mishra et al. average the outputs produced by two models, which have the same deep convolution network architecture but are trained using different optimizers (Adam and Nadam), for ASD classification based on s-MRI inputs.[13] Sharif et al. employ a pre-trained VGG16 model for ASD classification using features extracted from corpus callosum and intracranial brain volume of s-MRI.[14] Wang et al. propose a transformer-based framework for ASD classification, which makes the extraction of both local and global information from

the s-MRI possible.[15] Obviously, ABIDE serves as a valuable benchmark for machine classification of ASD based on s-MRI, however, the age of participants in ABIDE dataset are all above 5-year-old, which makes early-stage (i.e., below 5-year-old) screening of ASD based on machine learning not very accessible, as machine learning models usually perform poorly on out-of-distribution predictions. Besides, most of these studies has mediocre classification accuracies, which may potentially be attributed to the heterogeneous data collected from different resources[16].

Few studies use s-MRI from other datasets for machine classification of ASD. Sarovic et al. develop a user-friendly multivariate statistical method for analyzing the s-MRI of 24 ASD participants (mean age \pm standard deviation: 30.6 ± 7.1 years) and 21 TC participants (28.2 ± 6.4 years).[17] Conti et al. extract features from s-MRI of 18 TC children (55 ± 13 months) and 26 ASD children (56 ± 11 months), and then perform multivariate analysis based on support vector machine binary classifiers.[18] Zhang et al. propose a Siamese verification model for ASD classification, where 30 ASD and 30 TC are randomly selected from NDAR dataset for the experiment with their longitudinal brain s-MRI at 6 and 12 months of age.[19, 20] Early-stage machine classification of ASD are conducted in some of those studies mentioned above; however, all these works have mediocre performance, with predictive accuracies 73.2% for ref. [17], 87% for ref. [19] and AUC 0.73 for ref. [18].

In this work, we adopt contrastive variational autoencoder (CVAE) to extract the ASD-specific features for ASD detection using 78 s-MRI data (42 ASD and 36 TC) collected from Shenzhen Children's Hospital. The age of the children involved in the study ranges between 0.92-4.83-year-old. The ASD-specific features are extracted from the CVAE after the training for ASD classification, the mean accuracies of which are constantly above 0.97 in different cross-validation scenarios. A transfer learning strategy is introduced as well for the scenario when high accuracy won't be achieved with extremely

limited amount of data. Besides the ASD classification, neuroanatomical interpretation is thoroughly conducted, to identify potential biomarkers that could help target clinical treatment for ASD. This work can serve as a good benchmark for ASD study in children based on s-MRI.

METHODS

Dataset. In this study, we obtained 78 structural MRI (s-MRI) from Shenzhen Children’s Hospital, where 42 (10 female) of them are ASD participants and 36 (19 female) of them are TC participants. Age (in years) ranges from 1.00 to 4.83 in ASD group and from 0.92 to 4.33 in TC group. The s-MRI used as inputs for the contrastive machine learning remain in native space, i.e., they are not post-processed using any specific brain templates and are normalized between 0 and 1 and then resampled to a resolution of 64x64x64 before being fed into the CVAE for feature extraction. While in *Neuroanatomical interpretation* section, the s-MRI are post-processed into features of different cortical regions: for children between 0-2-year-old, the children’s s-MRI are processed by the Infantfreesurfer[21] tools, based on the per-month strategy (i.e., the 0-2-year-old are divided into 24 intervals, with each interval representing the length of a month, and children’s s-MRI within each interval are processed separately); for children between 2-5-year-old, the children’s s-MRI are first projected onto the age-specific brain templates to create the prior masks using ANTs[22], and then are further processed by Freesurfer[23] tool; the Freesurfer tools automatically parcellate the cortex and assign a neuroanatomical label to each location of the cortex (i.e., gray matter) based on probabilistic information, and the cortex is divided into 34 regions in this study based on Desikan-Killiany atlas[24]; *surface area* of each cortical region is measured as the feature indicating its uniqueness. All data used in this study are approved by local Internal Review Boards and carried out in accordance with ethics guidelines and regulations, and informed consents are obtained from all participants, or parent/legal guardians if participants are under 18.

Contrastive variational autoencoder (CVAE). The CVAE[25, 26] is used in our work to extract ASD-specific features as well as common shared features. It is a probabilistic-latent-variable model applied to contrastive analysis, which uses specific and shared feature extraction networks to emphasize the latent features of interest while suppressing uninteresting features in the data. As shown in **Figure 1**, the CVAE model consists of two encoders with identical architectures to extract ASD-specific and common shared features separately, and one shared decoder to reconstruct s-MRI of participants' brains. The encoder each has two convolutional layers (kernel size: 3, stride: 2, filters: 64 and 128 respectively) and two modules each consisting of two fully connected layers, where the first layers (both with 128 output nodes and Relu activation operation) in both modules are shared for the final extraction of the mean values (denoted as μ) and variance values (denoted as σ) of the features separately in the second layers (both with 16 output nodes). The decoder has two fully connected layers both with Relu operation (128 and 524288 output nodes respectively) and three deconvolutional layers (kernel size: 3, stride: 2, filters: 32, 16 and 1 respectively). The s-MRIs of TC participants pass through the shared feature encoder only, while the s-MRIs of ASD participants pass through both ASD-specific and shared feature encoders, which learn the distribution (mean and variance) of the features. The dimensions of both ASD-specific features and common shared features are 16. When reconstructing ASD brains, both common shared features and ASD-specific features (sampled from the features distribution learned from the encoders) are fed into the decoder, while reconstructing TC brains, only common shared features are sampled and then concatenated with 16 zeros as inputs for the same decoder.

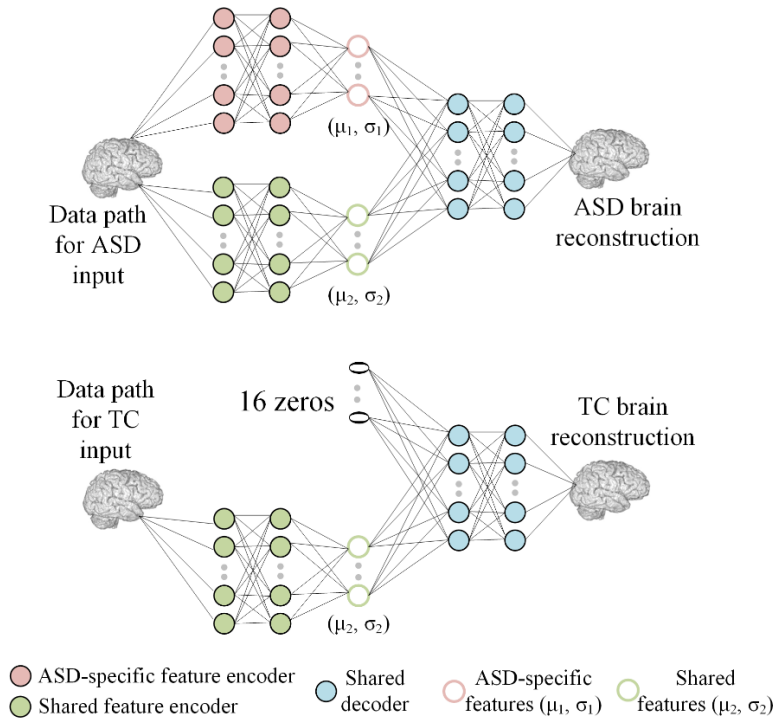


Figure 1. Contrastive variational autoencoder for extracting ASD-specific features and common shared features.

Implementation details. All 78 s-MRI data (reshaped as 64x64x64) from Shenzhen Children’s Hospital are leveraged for training CVAE, with Adam [23] adopted, where the parameters of the *learning rate*, *beta1*, *beta2* and *epsilon* are set as 1e-3, 0.9, 0.999 and 1e-7 respectively. The training batch size is 8, which means that for each iteration of training, 8 s-MRI of ASD participants and 8 s-MRI of TC participants, randomly sampled from the population, are fed into the network for learning. The training ends when the mean-square-error between input s-MRI and reconstructed s-MRI falls below (0.0005 for *ASD-specific features for ASD classification* section, 0.005 for *Transfer learning study of ABIDE-I* section). The experiments are conducted using Python 3.7 environment with the TensorFlow 1.13 framework and accelerated by 2 GPU cards.

RESULTS

ASD-specific features for ASD classification. According to the methods mentioned in *Contrastive variational autoencoder* section, the ASD participant can be represented by the ASD-specific features and common shared features, where the ASD-specific features reveal the irregular brain developments that never happen in the TC participants, thus serving the purpose of classifying ASD. We first evaluate the quality of ASD-specific features in ASD classification, and the results are shown in **Figure 2**. The ASD participants are either represented by ASD-specific features or common shared features, while the TC participants are represented by the common shared features. A random forest [27] model (with number of trees set to 100) is introduced to classify whether a participant is ASD or TC based on the features defined above, and the classification accuracies are measured in K-fold cross-validations. We try different K-fold numbers to create varying train/test scenarios, so that the comparison between ASD-specific features and common shared features are more robust. According to **Figure 2a**, the classification accuracy is much better improved when ASD-participants are represented using ASD-specific features, however the K-fold number changes. Besides, it's also understandable that increment of K-fold number leads to increment of variance in classification accuracy (characterized by the error bar in **Figure 2a**), since there are more test scenarios when K-fold number is larger. In **Figure 2b**, we evaluated the classification accuracies' dependence on sample size. For a specific sample size, e.g., 10, we sample 10 s-MRI out of the total 78 and then we train a classification random forest on it to get the accuracy, where the ASD participants are represented using ASD-specific features. We repeat it for 100 times to get the error bar of classification accuracy (measured via standard deviation), to capture the uncertainty of classification accuracy's dependence on sample size. The classification accuracy increases as sample size increases, which is intuitive since more data brings in more information. However, according to another study that classifies ASD via s-MRI features,[16] negative relationship is observed between sample size and classification accuracy, which is attributed to the varying data quality caused by heterogeneous data resources. Relatively speaking, the results of **Figure 2b** demonstrates a uniform data-quality distribution

of data used here. To visually characterize the superiority of ASD-specific features in ASD classification, we visualize the common shared features of ASD participants in **Figure 2c** and the ASD-specific features of ASD participants in **Figure 2d**, with common shared features of TC participants as the backgrounds in both plots. The ASD-specific features and common shared features of ASD participants and common shared features of TC participants are both in high dimension originally, we use t-SNE[28] visualization technique to project them onto 2-D space. From **Figure 2c** and **2d**, the ASD participants represented by ASD-specific features can be clearly separated from TC participants, while ASD participants represented by common shared features overlap well with TC participants.

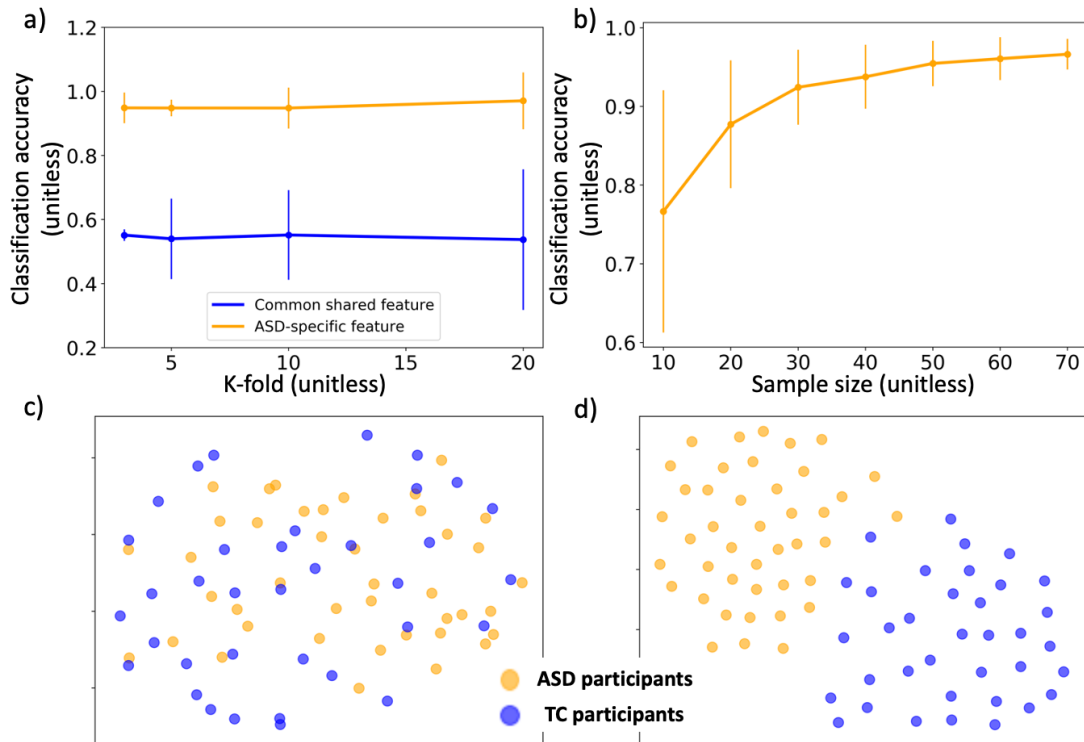
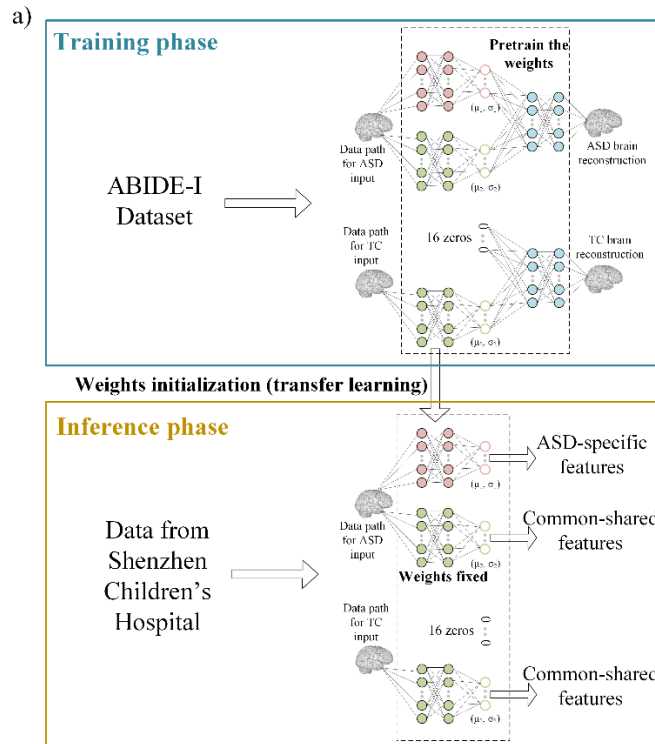


Figure 2. a) accuracy of classifying ASD with ASD participants being represented either by ASD-specific features or common shared features; b) relationship between classification accuracy and sample size, the accuracy of classifying ASD was measured based on ASD participants being represented by ASD-specific features; visualizing ASD participants and TC participants in 2-D feature space with TC

participants being represented by common share features while ASD participants being represented by either c) common shared features, or d) ASD-specific features.

Transfer learning study of ABIDE-I. Collecting high-quality s-MRI data for ASD study in children is both technically and ethically difficult, especially for children under age six,[29, 30] thus leading to a small dataset for exploration. As can be seen from the **Figure 2b**, the average classification accuracy can't reach 0.90 when the size of data was below 30, causing a less predictive model. A commonly adopted approach to improving the predictive accuracy on a specific task with limited data is to transfer the knowledge learned from a similar task with bigger data to that specific task, often noted as transfer learning.[31, 32] ABIDE-I[4] is an open-sourced database containing well-recorded s-MRI for both ASD and TC participants, the knowledge of which can be potentially transferred to improve the classification accuracy of ASD detection in our work. We collect 982 s-MRI from ABIDE-I, consisting of 470 ASD participants (age range 7-64 years) and 512 TC participants (age range 6-56 years), which are further used to train the contrastive variational autoencoder model, named as M_{ABIDE} . After the training, the ASD participants from Shenzhen Children's Hospital are passed through the M_{ABIDE} to acquire the ASD-specific features, and the TC participants from Shenzhen Children's Hospital are passed through the M_{ABIDE} to acquire common shared features. Only the ASD-specific features for ASD participants are explored here, as it's been demonstrated to be the predictive power for classifying ASD in the above section. The same random forest model is also trained to classify ASD for children in our work based on the features extracted from M_{ABIDE} , whose classification accuracy is tagged with "with transfer learning", as indicated in **Figure 3b** and **c**. The K-fold number and sample size analysis are also conducted here, and the corresponding classification accuracies from **Figure 2a** and **b** are recorded in **Figure 3b** and **c**, tagged with "without transfer learning". In **Figure 3b**, the accuracy of ASD classification based on ASD-specific features is improved by transfer learning, regardless of K-fold numbers. Besides, as can be seen from **Figure 3c**, the classification accuracy is less sensitive to data size after the transfer learning, and the

model is highly predictive even with small training data. When visualizing ASD participants based on common shared features in **Figure 3d** and ASD-specific features in **Figure 3e**, with both TC participants as the background, we can see that the ASD participants and TC participants still overlap well with each other when both being represented using common shared features but the boundary between ASD participants and TC participants is clearer when ASD participants are represented by ASD-specific features (i.e., the ASD participants are perfectly separated from TC participants), explaining why the classification accuracy is perfectly 1.00 in **Figure 3b**, regardless of K-fold numbers. From this study, ABIDE-I can be considered as a good source task for transfer learning, in terms of extracting effective features for classifying ASD in children. The other open-sourced databases may be explored and considered for similar purposes.



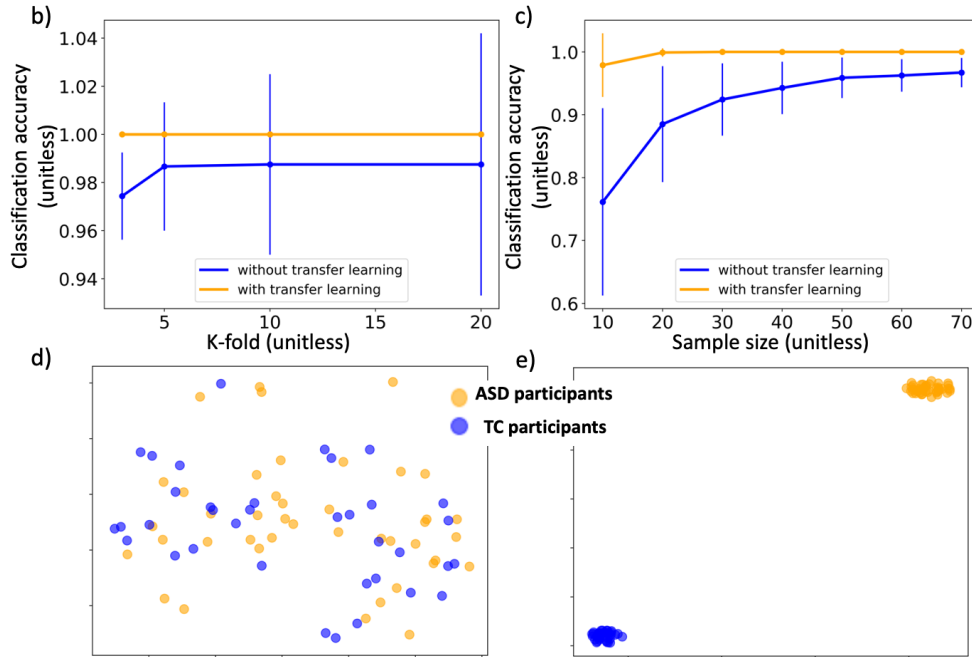


Figure 3. a) the schematic diagram of transfer learning study of ABIDE-I; b) accuracy of classifying ASD w/wo transfer learning, where ASD participants are represented by ASD-specific features; c) relationship between classification accuracy and sample size w/wo transfer learning, where ASD participants are represented by ASD-specific features; visualizing ASD participants and TC participants in 2-D feature space with TC participants being represented by common shared features while ASD participants being represented by either d) common shared features, or e) ASD-specific features.

Neuroanatomical interpretation. Although the ASD-specific features have high predictive power in classifying ASD, they don't explicitly tell which regions they correspond to in the brain, causing no sense of interpretation. Knowing the specific brain regions associating with ASD is critical for ASD intervention in the future, as they serve as the potential biomarkers that can help target clinical treatment.[33] To find the specific brain regions associating with ASD-specific features, we correlate them to the *surface area* that are manually extracted from the segmented cortex based on a specific atlas

(more details can be checked at *Dataset* section). The different cortical regions are responsible for different functions,[34] and the malfunction of certain regions may lead to the behavior of ASD. The cortex of children used in this study are first segmented into 34 regions, naming *temporalpole*, *bankssts*, *rostralanteriorcingulate*, *supramarginal*, *inferiorparietal*, *posteriorcingulate*, *parsopercularis*, *lateralorbitofrontal*, *middletemporal*, *entorhinal*, *frontalpole*, *parstriangularis*, *paracentral*, *lateraloccipital*, *parahippocampal*, *inferiortemporal*, *pericalcarine*, *caudalmiddlefrontal*, *cuneus*, *lingual*, *fusiform*, *superiorfrontal*, *transversetemporal*, *superiortemporal*, *medialorbitofrontal*, *isthmuscingulate*, *precuneus*, *caudalanteriorcingulate*, *precentral*, *parsorbitalis*, *rostralmiddlefrontal*, *postcentral*, *insula*, *superiorparietal*. We don't explore the functions of all the segmented regions here, rather focusing on the specific regions that distinguish ASD participants from TC participants most. We use representational similarity analysis (RSA)[35] to test whether the ASD-specific features/common shared features correlate with *surface area* of segmented cortical regions. We first calculate the pair-wise dissimilarity between participants with respect to the ASD-specific features and common shared features separately and obtain two groups of dissimilarity matrixes. Specifically, 42 s-MRIs of ASD participants from Shenzhen Children's Hospital are passed through two encoders of the trained CVAE models separately, then 42 ASD-specific features (42 x 16) and 42 common shared features (42 x 16) are generated by sampling from the encoded feature distributions. We calculate the pairwise Euclidean distances between ASD-specific features and between common shared features, which form two dissimilarity matrixes (42×42) respectively. We sample 10 times from each encoded feature distribution and two groups of dissimilarity matrixes (10 for ASD-specific features and 10 for common shared features) are generated with method mentioned above. We then repeat this process for *surface area* of each segmented cortical region of ASD participants. Finally, we correlate the dissimilarity matrices of ASD-specific features/common shared features to the dissimilarity matrices of each cortical region's *surface area* using the Kendall rank correlation coefficient (Kendall τ) [36], a measurement (value between -1 and 1) between two rankings \mathbf{X} (x_1, x_2, \dots, x_n) and \mathbf{Y} (y_1, y_2, \dots, y_n) using the formula: $(P - Q) / \sqrt{((P + Q + T) \times (P + Q + U))}$, where P

is the number of concordant pairs ($x_i > x_j$ & $y_i > y_j$ or $x_i < x_j$ & $y_i < y_j$), Q the number of discordant pairs ($x_i > x_j$ & $y_i < y_j$ or $x_i < x_j$ & $y_i > y_j$), T the number of ties only in **X**, and U the number of ties only in **Y**. If a tie occurs for the same pair in both **X** and **Y**, it is not added to either T or U. Values close to 1 indicate strong agreement of the correspondence between two rankings, while values close to -1 indicate strong disagreement. The significance of a relationship is characterized by p-value, with p-value smaller than 0.05 as significant. We pay attention to the cortical regions, where ASD-specific features have positive correlations and common shared features have negative correlations, both statistically significant. In other words, those cortical regions indicate the biggest brain differences between ASD participants and TC participants involved in our study. Based on **Figure 4**, the names of cortical regions that can distinguish ASD participants from TC participants most, are *supramarginal* and *inferiortemporal*, and we name those regions *ASD-specific-regions*. The names and functions of *ASD-specific-regions* are recorded in **Table 1**. Based on **Table 1**, the malfunctions of *ASD-specific-regions* will make impact on your interpretation of spoken language as well as written language (phonological decisions and visual word recognition) and your recognition of objects in the environment (visual recognition of objects), which will further lead to social communication/interaction disorders. ASD is a complex group of developmental disorders characterized by difficulties in social communication/interaction that can persist throughout life,[37, 38] and the *ASD-specific-regions* found above indicate where those problems come from in the brain, which serve as reasonable biomarkers that could help target treatment.

Table 1. Names and functions of the areas that distinguish ASD participants from TC participants most in our study.

Name of area	Function of area
<i>supramarginal</i> [39, 40]	phonological decisions and visual word recognition
<i>inferiortemporal</i> [41]	visual recognition of objects

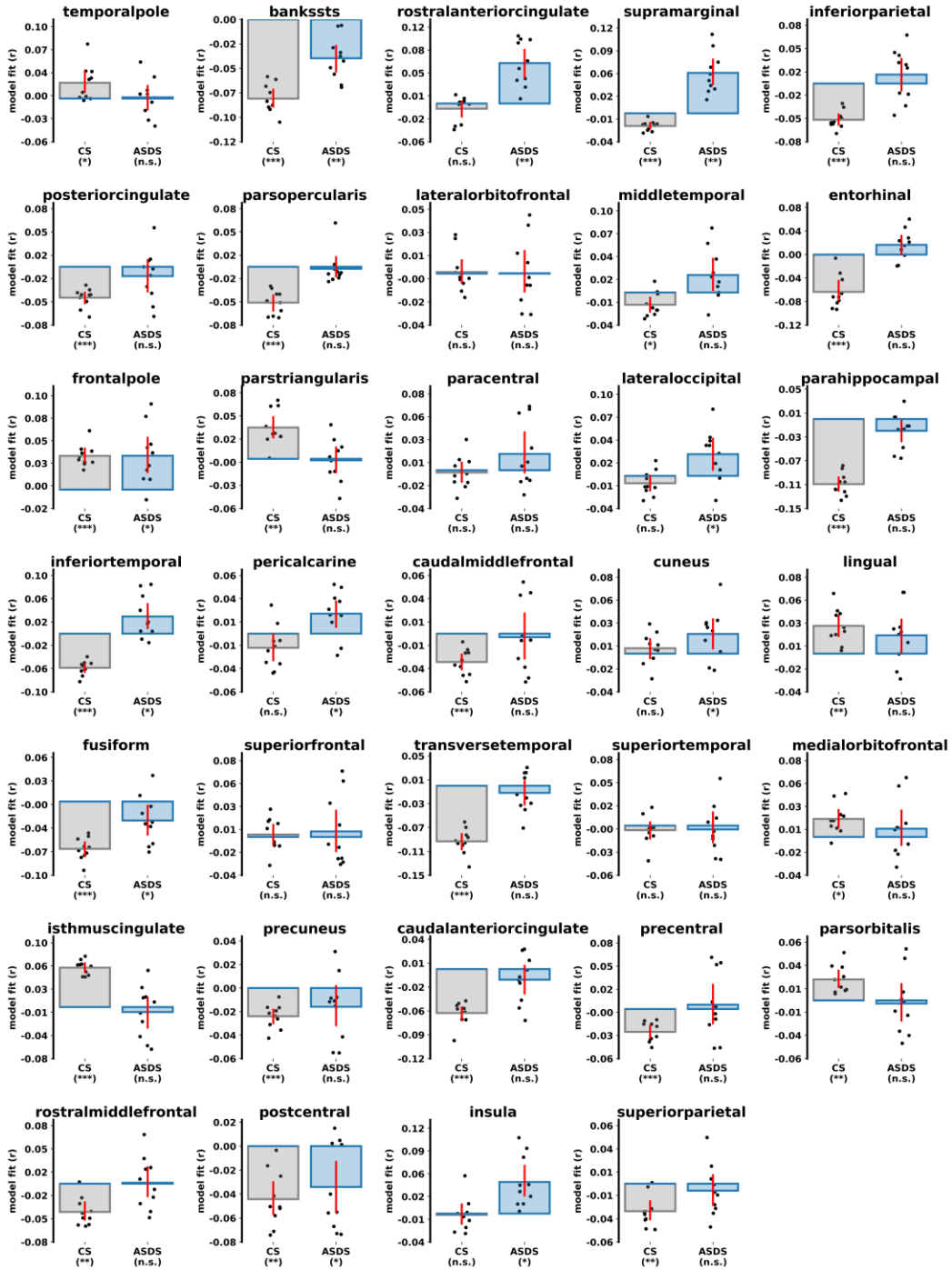


Figure 4. Kendall rank correlation coefficient (Kendall τ) measuring agreement/disagreement between the dissimilarity matrices of ASD-specific (ASDS) features /common shared (CS) features and the matrices for each cortical region's *surface area*. The “n.s.”, “*”, “**”, and “***” correspond to p-value of 1.0, 0.05, 0.001, and 0.0001.

CONCLUSION & DISCUSSION

In summary, we conduct machine classification of ASD in children based on s-MRI features extracted using CVAE and achieve a stable predictive accuracy above 0.97 under different cross-validation scenarios. The predictive accuracy of the classification model is sensitive to data size, which will be degraded when lowering the data size. To mitigate the impact of data size on the predictive accuracy, we introduce a transfer learning strategy, which learns the knowledge from ABIDE-I dataset and transfers the learned knowledge to improve the classification accuracy here when data is extremely limited (below 30). As demonstrated, the transfer learning works effectively towards making predictive accuracy less sensitive to data size. Finally, we conduct neuroanatomical interpretation to disclose the specific cortical regions correlated to ASD, which may help find potential biomarkers for ASD treatments.

DATA AVAILABILITY STATEMENT

Code and data will be available at https://github.com/RUIMINMA1996/ASD_GM upon the publication of this work but are available from the corresponding author on reasonable request.

ACKNOWLEDGEMENT

The authors acknowledge the financial support from Shenzhen Science and Technology Program under grant no. KQTD20200820113106007, Shenzhen Key Laboratory of Intelligent Bioinformatics (ZDSYS20220422103800001), Shenzhen Basic Research Fund under grant no. RCYX20200714114734194, Key Research and Development Project of Guangdong Province under grant no. 2021B0101310002, National Science Foundation of China under grant no. 62272449. We would also like to thank the funding support by the Youth Innovation Promotion Association(Y2021101), CAS to

Yanjie Wei. The computation was supported by the Sugon computing platform under the grant no. KQTD20200820113106007.

AUTHOR CONTRIBUTIONS STATEMENT

Ruimin Ma: Conceptualization, Data analyzing, Methodology, Writing-original draft, Software. **Ruitao Xie:** Writing-original draft, Software. **Yanlin Wang:** Data curation. **Jintao Meng:** Writing-Reviewing and Editing. **Yanjie Wei:** Supervision, Funding, Writing-Reviewing and Editing. **Yi Pan:** Supervision, Funding, Writing-Reviewing and Editing.

COMPETING INTERESTS

The authors declare that they have no competing interests.

ETHICS APPROVAL AND CONSENT TO PARTICIPATE

Not applicable.

CONSENT FOR PUBLICATION

Not applicable.

REFERENCE

1. Lord, C., Elsabbagh, M., Baird, G. and Veenstra-Vanderweele, J., *Autism spectrum disorder*. The lancet, 2018. **392**(10146): p. 508-520.
2. Thabtah, F.a.P., D., *A new machine learning model based on induction of rules for autism detection*. Health informatics journal, 2020. **26**(1): p. 264-286.
3. Moridian, P., Ghassemi, N., Jafari, M., Salloum-Asfar, S., Sadeghi, D., Khodatars, M., Shoeibi, A., Khosravi, A., Ling, S.H., Subasi, A. and Abdulla, S.A., *Automatic autism spectrum disorder detection using artificial intelligence methods with MRI neuroimaging: A review*. arXiv preprint arXiv, 2022. **2206**(11233).
4. Di Martino, A., Yan, C.G., Li, Q., Denio, E., Castellanos, F.X., Alaerts, K., Anderson, J.S., Assaf, M., Bookheimer, S.Y., Dapretto, M. and Deen, B., *The autism brain imaging data exchange: towards a large-scale evaluation of the intrinsic brain architecture in autism*. Molecular psychiatry, 2014. **19**(6): p. 659-667.
5. Di Martino, A., O'connor, D., Chen, B., Alaerts, K., Anderson, J.S., Assaf, M., Balsters, J.H., Baxter, L., Beggiano, A., Bernaerts, S. and Blanken, L.M., *Enhancing studies of the connectome in autism using the autism brain imaging data exchange II*. Scientific data, 2017. **4**(1): p. 1-15.
6. Kong, Y., Gao, J., Xu, Y., Pan, Y., Wang, J. and Liu, J., *Classification of autism spectrum disorder by combining brain connectivity and deep neural network classifier*. Neurocomputing, 2019. **324**: p. 63-68.
7. Hiremath, Y., Ismail, M., Verma, R., Antunes, J. and Tiwari, P., *Combining deep and hand-crafted MRI features for identifying sex-specific differences in autism spectrum disorder versus controls*. In Medical Imaging 2020: Computer-Aided Diagnosis, 2020, March. **11314**: p. 445-451.
8. Rohlfing, T., Zahr, N.M., Sullivan, E.V. and Pfefferbaum, A., *The SRI24 multichannel atlas of normal adult human brain structure*. Human brain mapping, 2010. **31**(5): p. 798-819.
9. Gao, J., Chen, M., Li, Y., Gao, Y., Li, Y., Cai, S. and Wang, J., *Multisite autism spectrum disorder classification using convolutional neural network classifier and individual morphological brain networks*. Frontiers in Neuroscience, 2021. **14**.
10. Zhou, B., Khosla, A., Lapedriza, A., Oliva, A. and Torralba, A., *Learning deep features for discriminative localization*. In Proceedings of the IEEE conference on computer vision and pattern recognition, 2016: p. 2921-2929.
11. Selvaraju, R.R., Cogswell, M., Das, A., Vedantam, R., Parikh, D. and Batra, D., *Grad-cam: Visual explanations from deep networks via gradient-based localization*. In Proceedings of the IEEE international conference on computer vision, 2017: p. 618-626.
12. Yang, R., Ke, F., Liu, H., Zhou, M. and Cao, H.M., *Exploring sMRI biomarkers for diagnosis of autism spectrum disorders based on multi class activation mapping models*. IEEE Access, 2021. **9**(124122-124131).
13. Mishra, M.a.P., U.C., *A classification framework for Autism Spectrum Disorder detection using sMRI: Optimizer based ensemble of deep convolution neural network with on-the-fly data augmentation*. Biomedical Signal Processing and Control, 2023. **84**.
14. Sharif, H.a.K., R.A., *A novel machine learning based framework for detection of autism spectrum disorder (ASD)*. Applied Artificial Intelligence, 2022. **36**(1): p. 2004655.
15. Wang, Z., Peng, D., Shang, Y. and Gao, J., *Autistic spectrum disorder detection and structural biomarker identification using self-attention model and individual-level morphological covariance brain networks*. Frontiers in Neuroscience, 2021.
16. Ma, R., Wang, Y., Wei, Y. and Pan, Y., *Meta-data Study in Autism Spectrum Disorder Classification Based on Structural MRI*. arXiv preprint arXiv, 2022. **2206**(05052).
17. Sarovic, D., Hadjikhani, N., Schneiderman, J., Lundström, S. and Gillberg, C., *Autism classified by magnetic resonance imaging: A pilot study of a potential diagnostic tool*. International journal of methods in psychiatric research, 2020. **29**(4): p. 1-18.

18. Conti, E., Retico, A., Palumbo, L., Spera, G., Bosco, P., Biagi, L., Fiori, S., Tosetti, M., Cipriani, P., Cioni, G. and Muratori, F., *Autism Spectrum Disorder and Childhood Apraxia of Speech: Early language-related hallmarks across structural MRI study*. Journal of personalized medicine, 2020. **10**(4).
19. Zhang, X., Ding, X., Wu, Z., Xia, J., Ni, H., Xu, X., Liao, L., Wang, L. and Li, G., *Siamese verification framework for autism identification during infancy using cortical path signature features*. In 2020 IEEE 17th International Symposium on Biomedical Imaging (ISBI), 2020, April: p. 1-4.
20. .
21. Zöllei, L., Iglesias, J.E., Ou, Y., Grant, P.E. and Fischl, B., *Infant FreeSurfer: An automated segmentation and surface extraction pipeline for T1-weighted neuroimaging data of infants 0–2 years*. Neuroimage, 2020. **218**.
22. Avants, B.B., Duda, J.T., Kilroy, E., Krasileva, K., Jann, K., Kandel, B.T., Tustison, N.J., Yan, L., Jog, M., Smith, R. and Wang, Y., *Large-scale evaluation of ANTs and FreeSurfer cortical thickness measurements*. Scientific Data, 2014. **2**.
23. FreeSurfer, F.B., *FreeSurfer*. NeuroImage, 2012. **62**(2): p. 774-781.
24. Desikan, R.S., Ségonne, F., Fischl, B., Quinn, B.T., Dickerson, B.C., Blacker, D., Buckner, R.L., Dale, A.M., Maguire, R.P., Hyman, B.T. and Albert, M.S., *An automated labeling system for subdividing the human cerebral cortex on MRI scans into gyral based regions of interest*. Neuroimage, 2006. **31**(3): p. 968-980.
25. Sevenson, K.A., Ghosh, S. and Ng, K., *Unsupervised learning with contrastive latent variable models*. In Proceedings of the AAAI Conference on Artificial Intelligence, 2019, July. **33**(01): p. 4862-4869.
26. Abid, A.a.Z., J., 2019. Contrastive variational autoencoder enhances salient features. arXiv preprint arXiv:1902.04601., *Contrastive variational autoencoder enhances salient features*. arXiv preprint arXiv, 2019. **1902**(04601).
27. Breiman, L., *Random forests*. Machine Learning, 2001. **45**(1): p. 5-32.
28. Van der Maaten, L.a.H., G., *Visualizing data using t-SNE*. Journal of machine learning research, 2008. **9**(11).
29. Aglinskis, A., Hartshorne, J.K. and Anzellotti, S., *Contrastive machine learning reveals the structure of neuroanatomical variation within autism*. Science, 2022. **376**(6597): p. 1070-1074.
30. Khadem-Reza, Z.K. and H. Zare, *Evaluation of brain structure abnormalities in children with autism spectrum disorder (ASD) using structural magnetic resonance imaging*. The Egyptian Journal of Neurology, Psychiatry and Neurosurgery, 2022. **58**(1).
31. Weiss, K., Khoshgoftaar, T.M. and Wang, D., *A survey of transfer learning*. Journal of Big data, 2016. **3**(1): p. 1-40.
32. Ma, R., Y.J. Colon, and T. Luo, *Transfer Learning Study of Gas Adsorption in Metal-Organic Frameworks*. ACS Appl Mater Interfaces, 2020. **12**(30): p. 34041-34048.
33. Goldani, A.A., Downs, S.R., Widjaja, F., Lawton, B. and Hendren, R.L., *Biomarkers in autism*. Frontiers in psychiatry, 2014. **5**.
34. Mercadante, A.A.a.T., P., *Neuroanatomy, Gray Matter*. 2020.
35. Kriegeskorte, N., M. Mur, and P. Bandettini, *Representational similarity analysis - connecting the branches of systems neuroscience*. Front Syst Neurosci, 2008. **2**: p. 4.
36. Abdi, H., *The Kendall rank correlation coefficient*. Encyclopedia of Measurement and Statistics, 2007. **Sage, Thousand Oaks, CA**: p. 508-510.
37. Association, D.-A.P., *Diagnostic and statistical manual of mental disorders*. Arlington: American Psychiatric Publishing, 2013. **10**.
38. Hyman, S.L., Levy, S.E., Myers, S.M., Kuo, D.Z., Apkon, S., Davidson, L.F., Ellerbeck, K.A., Foster, J.E., Noritz, G.H., Leppert, M.O.C. and Saunders, B.S., *Identification, evaluation, and management of children with autism spectrum disorder*. Pediatrics, 2020. **145**(1).

39. Hartwigsen, G., Baumgaertner, A., Price, C.J., Koehnke, M., Ulmer, S. and Siebner, H.R., *Phonological decisions require both the left and right supramarginal gyri*. Proceedings of the National Academy of Sciences, 2010. **107**(38): p. 16494-16499.
40. Stoeckel, C., Gough, P.M., Watkins, K.E. and Devlin, J.T., *Supramarginal gyrus involvement in visual word recognition*. Cortex, 2009. **45**(9): p. 1091-1096.
41. Miyashita, Y., *Inferior temporal cortex: where visual perception meets memory*. Annual review of neuroscience, 1993. **16**(1): p. 245-263.